AIAA JOURNAL
Vol. 46, No. 1, January 2008

Variable Kinematic Model for the Analysis of Functionally Graded Material Plates

E. Carrera,* S. Brischetto,† and A. Robaldo
Politecnico di Torino, 10129 Turin, Italy

DOI: 10.2514/1.32490

This work addresses the static analysis of functionally graded material plates subjected to transverse mechanical loadings. The unified formulation and principle of virtual displacements are employed to obtain both closed-form and finite element solutions. The use of the unified formulation permits a large variety of plate models with variable kinematic assumptions to be compared in the same framework. These differ according to the order of the expansion in the thickness direction and the variable description: the order of the expansion ranges from 1 to 4, thus covering first-order as well as higher-order theories; the description of the unknowns can be equivalent single layer or layerwise. The dependence of the material data on the thickness direction was introduced by employing thickness functions that are derived from the Legendre polynomials that are used in the layerwise case. The proposed approach is independent of the used transition function, and as a result, any continuous variations of the material properties in the thickness direction may be easily implemented. The obtained solutions (closed form and finite element) are validated through comparison with three-dimensional exact solutions and other available solutions. These show the limitations of classical plate theories as well as the convenience of the use of the proposed variable kinematic models for the analysis of functionally graded material plates.

Nomenclature

A_k	=	integration domain in the z direction
$\boldsymbol{a}$	=	vector generic variable
a_k	=	dimension of the plate in the x direction
b	=	bottom of the layer or plate
b_k	=	dimension of the plate in the y direction
C	=	constitutive equations
C_{ij}	=	material stiffnesses
$\boldsymbol{C}_r$	=	weighted stiffness matrix for functionally graded material
$\boldsymbol{C}_{pp}, \boldsymbol{C}_{pn}, \boldsymbol{C}_{np}, \boldsymbol{C}_{nn}$	=	material stiffness subarrays
$\boldsymbol{C}(z)$	=	stiffness matrix for functionally graded material
$\boldsymbol{C}_0$	=	reference stiffness matrix
$\boldsymbol{D}_p, \boldsymbol{D}_{np}, \boldsymbol{D}_{nz}$	=	differential operator matrices
E_i	=	Young's moduli
$E_{\tau sr}, E_{\tau,zsr}, E_{\tau s,zr}, E_{\tau,zs,zr}$	=	integrals in the z direction
F_r	=	thickness function for the functionally graded material properties
F_s	=	thickness function for the variation
F_τ	=	thickness function for the variable
G	=	geometrical relations
$\boldsymbol{g}(z)$	=	function for the variation of functionally graded material properties in the z direction
G_{ij}	=	shear moduli
h_k	=	thickness layer
$\boldsymbol{I}_p, \boldsymbol{I}_{np}$	=	additional arrays to perform integration by parts
$\boldsymbol{K}_{uu}^{k\tau srij}, \boldsymbol{K}_{up}^{k\tau srij}$	=	fundamental nuclei for functionally graded material
k	=	layer index
κ	=	volume fraction exponent
l	=	higher-order terms
m	=	waves number in the x direction
N	=	order of expansion in the thickness direction
N_i, N_j	=	shape functions
N_l	=	number of layers
N_{ml}	=	number of mathematical layers
N_n	=	number of nodes
N_r	=	order of expansion for functionally graded material properties
n	=	waves number in the y direction
P_j	=	Legendre's polynomials
$P_{u\tau}^k$	=	external load
$q_{\tau j}$	=	nodal values
T	=	transposed vector
t	=	top of the plate or layer
$\hat{U}_{x\tau}^k, \hat{U}_{y\tau}^k, \hat{U}_{z\tau}^k$	=	displacement amplitudes
$\boldsymbol{u}$	=	displacement vector
u_x, u_y, u_z	=	displacement components in the x, y and z directions
x, y, z	=	coordinates reference system
z_k	=	local thickness coordinate
Γ_k	=	edge of surface Ω_k
γ	=	inhomogeneity parameter
$\delta\boldsymbol{a}$	=	vector for the variation of a generic variable
δL_e^k	=	external work
ϵ_p, ϵ_n	=	in-plane and normal/transverse strains
ζ_k	=	nondimensional thickness coordinate
ν_{ij}	=	Poisson's ratio
$\boldsymbol{\Pi}_{uu}^{k\tau sr}$	=	matrix to perform boundary conditions
σ_p, σ_n	=	in-plane and normal/transverse stresses
Ω_k	=	in-plane integration domain
$\lhd \ldots \rhd_{\Omega_k}$	=	integrate over the element domain

Received 30 May 2007; revision received 21 August 2007; accepted for publication 22 August 2007.

*Professor, Aerospace Structures and Aeroelasticity, Aerospace Department, Corso Duca degli Abruzzi 24.

†Ph.D. Student; salvatore.brischetto@polito.it (Corresponding Author).

I. Introduction

AN ADVANTAGE of functionally graded materials (FGMs) over laminated composites is that the material properties vary continuously in an FGM (Fig. 1 indicates the reference system for a generic plate, and Fig. 2 shows the case of transition from full

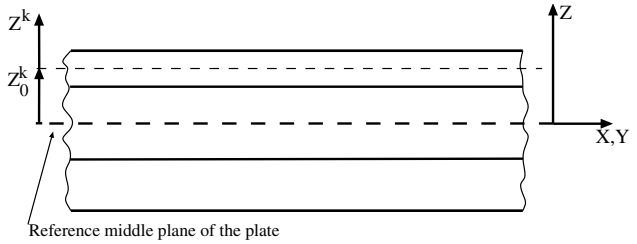

Fig. 1 Coordinate system along the thickness of the plate.

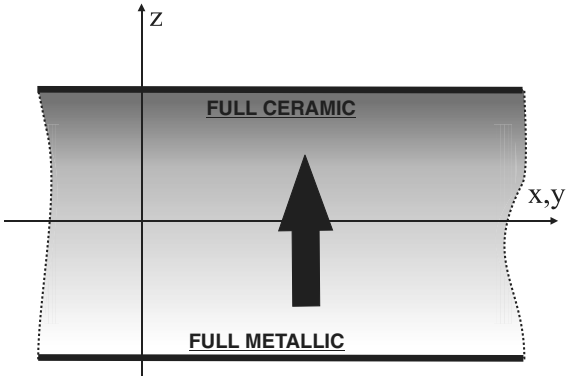

Fig. 2 Example of a single-layered FGM plate.

ceramic to full metallic materials) as opposed to being discontinuous across adjoining layers in laminated composites. The volume fraction of the constituent FGMs changes gradually in only the thickness direction and the elastic properties depend on the z coordinate. FGMs have been presented as an alternative to laminated composite materials that show a mismatch in properties at the material interfaces. This material discontinuity in laminated composite materials leads to large interlaminar stresses and the possibility of the initiation and propagation of cracks [1]. Another possible configuration (Fig. 3) is the use of an FGM interlayer that links layers with very different mechanical properties.

An accurate kinematic description of the problem variables in the thickness direction appears to be as a key point for the analysis of the mechanical behavior of FGM plates. Many works on FGM plates have recently appeared. An overview of some of these is given in the following text.

A three-dimensional solution for FGM plates subjected to a transverse mechanical load was proposed in the work by Kashtalyan [2]. The shear modulus changes exponentially through the thickness direction and the Poisson ratio is constant. The transverse displacement u_z is obtained for different values of the inhomogeneity parameter γ, and in-plane and out-plane stresses are evaluated through the thickness direction.

Zenkour [3] accounted for the static response of a simply supported functionally graded rectangular plate subjected to a transversal mechanical load. A generalized shear deformation theory is used that neglects transversal normal strains. The material properties of the plate are assumed to be graded in the thickness direction, according to a simple power-law distribution, in terms of the volume fractions of the constituents (metallic and ceramic). The displacement and stress values are reported for different values of the exponential κ, which ranges from full ceramic to full metallic.

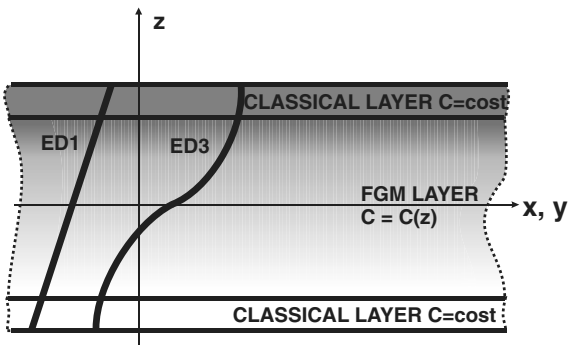

Fig. 3 Example of a multilayered plate with an internal FGM layer with through-the-thickness distribution of displacement u for the equivalent-single-layer model.

Batra and Jin [4] considered FGM plates that are obtained by changing the fiber orientation in the thickness coordinate z. A free-vibrations problem is studied via a finite element (FE) method. A first-order shear deformation theory is applied and different boundary conditions are investigated: all edges clamped, all edges simply supported, two opposite edges clamped and the other two free, and so on. A comparison with a 10- and a 20-discrete-layer methodology is accomplished for the first 10 frequencies.

Qian et al. [5] analyzed the static deformations and free and forced vibrations of a thick rectangular functionally graded elastic plate using a high-order shear and normal deformable plate theory and a meshless local Petrov–Galerkin method. The plate material, made of two isotropic constituents, is assumed to be macroscopically isotropic with material properties only varying in the thickness direction. The effective material moduli are computed using the Mori–Tanaka homogenization technique in [6]. Ramirez et al. [7] presented a static analysis of an anisotropic elastic plate composed of functionally graded materials. The solution was obtained using a discrete layer theory (20 or 30 layers) in combination with the Ritz method. Two types of FGM laws were considered: an exponential variation of the mechanical properties through the thickness of the plate and mechanical properties as a function of the fiber orientation, which varies quadratically through the laminate thickness. The FE method solution was compared with the exact solution by Pan [8] for a functionally graded rectangular composite laminate under simply supported edge conditions; Pan's solution extends Pagano's [9,10] 3D solution to functionally graded materials and it could therefore degenerate into Pagano's solution when the elastic properties are constant through the thickness direction.

A three-dimensional exact solution is presented for free and forced vibrations of simply supported FGM rectangular plates in [11]. Thick and thin plates were analyzed for arbitrary variations of the material properties in the thickness direction. The effective material properties are estimated by either the Mori-Tanaka or the self-consistent schemes. Exact natural frequencies, displacements, and stresses are used to assess the accuracy of the classical lamination theory (CLT), the first-order shear deformation theory (FSDT), and a third-order shear deformation theory.

An analytical solution for thermomechanical deformations of a simply supported FGM plate subjected to time-dependent thermal loads on its top and/or bottom surfaces is illustrated in [12]. The uncoupled quasi-static linear thermoelasticity theory is adopted in which the change in temperature, if any, due to deformations is neglected.

In [13], a third-order shear deformation theory is applied to the static analysis of an FGM plate. The plate material is made of two isotropic constituents with their volume fractions varying only in the thickness direction. The aspect ratio effects of the plate and the volume fractions of the constituents on the centroidal deflection are scrutinized.

An elastic, rectangular, and simply supported functionally graded material plate of medium thickness subjected to transverse loading was investigated in [14,15]. Three evaluations are considered in z for the FGM properties: the volume fraction can be defined by a power-law, sigmoid, or exponential function; Poisson's ratio is considered constant. The model is based on CLT and Fourier series expansion. Closed-form solution is illustrated in [14], and a comparison between FE and analytical solutions is given in [15].

The free-vibration problem of FGM plates is presented in the case of magnetoelectroelastic fields in [16]. The material exponential laws are used for elastic property and fiber orientation. Natural frequencies are determined using a discrete layer model with two different approaches. In the first approach, the functions describing the gradation of the material properties through the thickness of the

plate are incorporated in the governing equations. In the second approach, the plate is divided into a finite number of homogeneous layers.

The extension of the unified formulation (UF) by Carrera [17,18] to FGM plates is proposed in the present paper. The UF has extensively been already applied for the mechanical [19,20], thermal [21,22], and piezoelectric [23–25] analysis of multilayered plates and shells. The generalized expansion, upon which the UF is based, relies on a set of functions herein indicated as thickness functions. In this manner, the unified formulation reduces a three-dimensional problem to a bidimensional one. At the same time, the order of expansion along the thickness of the plate is taken as a free parameter of the problem and it can be changed in the interval ranging from 1 to 4. By appropriately choosing the thickness functions, either an equivalent-single-layer (ESL) or a layerwise (LW) description along the thickness of the plate is admissible. In an ESL model, a global assumption for the unknowns is made along the thickness of the plate, whereas in a LW model, the expansion applies to each layer separately and then interlaminar continuity conditions are enforced. As a result, an exhaustive variable kinematic model is obtained.

The accuracy of the proposed variable kinematic model for the analysis of an FGM layer lies in its capability to describe the continuous variations of the material characteristics (either mechanical, thermal, or electrical) along the thickness. The extension of the UF to FGM is quite straightforward because the main idea is to apply the same expansions used for the primary variables to the material characteristics. The present article mainly focuses on the extension of the capabilities of the UF to analyze FGM layers, and a few numerical results are given related to single-layer FGM plates. The model has, however, been prepared for future benchmark studies that could consider multilayer structures with embedded FGM layers.

The paper is organized as follows. The UF is presented in general in Sec. II for multilayered structures (with the possibility of considering a LW or ESL model); Sec. III illustrates the procedure that extends the UF to FGM layers. The governing equations and fundamental nuclei are given in Sec. IV for both the closed-form (CF) solution and FE method. Numerical assessments are made in Sec. VI.

II. Unified Formulation

The application of a two-dimensional method for plates permits us to express the unknown variables as a set of thickness functions depending only on the thickness coordinate z and the correspondent variable depending on the in-plane coordinates x and y.

The unified formulation is a technique that handles a large variety of plate/shell modeling in a unified manner. According to UF, the governing equations are written in terms of a few fundamental nuclei that do not formally depend on the order of expansion N used in the z direction or a description of variables (LW or ESL).

The generic variable $\boldsymbol{a}(x, y, z)$ (for instance, a displacement) and its variation $\delta\boldsymbol{a}(x, y, z)$ are written according to the following general expansion:

$$\begin{aligned} \boldsymbol{a}(x, y, z) &= F_\tau(z)\boldsymbol{a}_\tau(x, y) \\ \delta\boldsymbol{a}(x, y, z) &= F_s(z)\delta\boldsymbol{a}_s(x, y) \quad \text{with} \quad \tau, s = 1, \ldots, N \end{aligned} \tag{1}$$

Bold letters denote arrays, (x, y) are the in-plane coordinates, and z is the thickness coordinate (see Fig. 1). The summing convention with repeated indexes τ and s is assumed. The order of expansion N goes from first to fourth order, and depending on the used thickness functions, a model can be ESL when the variable is assumed for the whole multilayer (see Fig. 3) and LW when the variable is considered independent in each layer (see Fig. 4). The use of a single FGM layer as an alternative to a sandwich structure was already introduced in Fig. 2. A further possibility is the use of a FGM between two layers that are made of materials that do not change their properties in the z direction, and these are denoted as classical layers in Figs. 3 and 4. The Fig. 2 configuration can be handled with the use of ESL, and the LW approach could be mandatory in the cases in Figs. 3 and 4 for particular conditions.

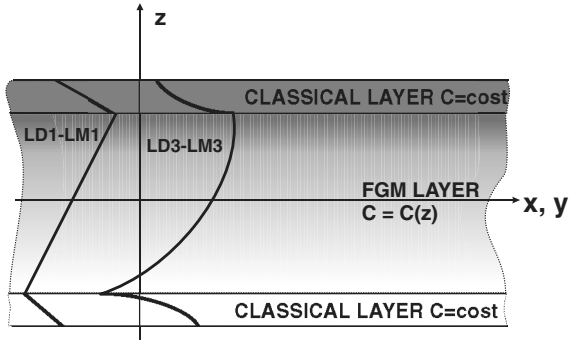

Fig. 4 Example of a multilayered plate with an internal FGM layer with through-the-thickness distribution of displacement u for the layerwise model.

A. Equivalent-Single-Layer Theories

The displacement $\boldsymbol{u} = (u_x, u_y, u_z)$ is described according to equivalent-single-layer description if the unknowns are the same for the whole plate. The assembling procedure for ESL in case of a multilayer structure with FGM layers and layers with constant elastic properties is indicated in Fig. 5. The stiffness matrices in case of FGM layers have a further assembling procedure that considers the elastic coefficients depending on z coordinate, as will be illustrated in Sec. III.

The z expansion is obtained via Taylor polynomials; that is,

$$\boldsymbol{u} = F_0\boldsymbol{u}_0 + F_1\boldsymbol{u}_1 + \cdots + F_N\boldsymbol{u}_N = F_\tau\boldsymbol{u}_\tau \quad \text{with} \quad \tau = 0, 1, \ldots, N \tag{2}$$

where N is the order of expansion that ranges from linear (1) to fourth (4) order:

$$F_0 = z^0 = 1, F_1 = z^1 = z, \ldots, F_N = z^N \tag{3}$$

B. Layerwise Theories

The layerwise approach describes the layers as independent plates. It is introduced according to the following expansion:

$$\boldsymbol{u}^k = F_t\boldsymbol{u}_t^k + F_b\boldsymbol{u}_b^k + F_l\boldsymbol{u}_l^k = F_\tau\boldsymbol{u}_\tau^k \tag{4}$$

where

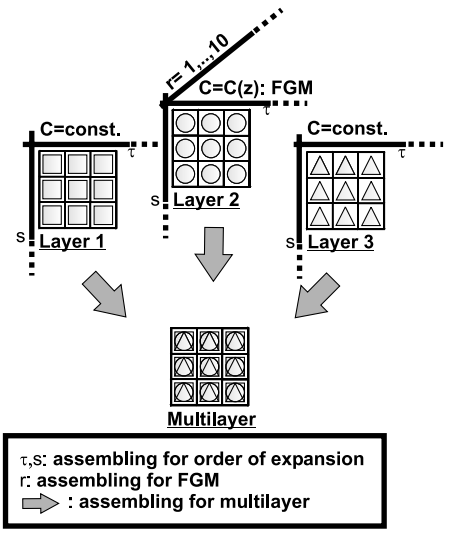

Fig. 5 Example of the assembling procedure in the case of the equivalent-single-layer model; the layers can be classical or FGM.

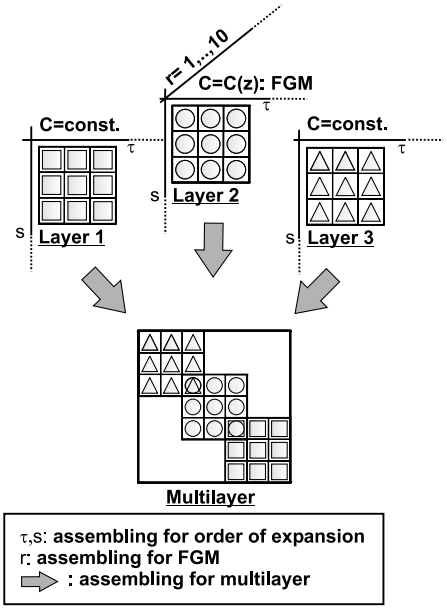

Fig. 6 Example of the assembling procedure in the case of the layerwise model; the layers can be classical or FGM.

$$\tau = t, b, l \quad \text{with} \quad l = 2, \ldots, N$$

The assembling procedure for LW in the case of a multilayer structure is indicated in Fig. 6. As in the ESL case, some layers could be of FGM type, and in this case, a further assembling on the r index is necessary. The top and bottom values are t and b, and l terms denote the higher-order terms of expansion. The thickness functions $F_\tau(\zeta_k)$ have now been defined at the k-layer level: they are a linear combination of Legendre polynomials $P_j = P_j(\zeta_k)$ of the jth order defined in the ζ_k domain [$\zeta_k = 2z_k/h_k$, with z_k local coordinate and h_k thickness, both referred to as the kth layer, so that $-1 \leq \zeta_k \leq 1$ (see Fig. 1)]. The first five Legendre polynomials are

$$\begin{aligned} P_0 &= 1, \qquad P_1 = \zeta_k, \qquad P_2 = \frac{\left(3\zeta_k^2 - 1\right)}{2} \\ P_3 &= \frac{5\zeta_k^3}{2} - \frac{3\zeta_k}{2}, \qquad P_4 = \frac{35\zeta_k^4}{8} - \frac{15\zeta_k^2}{4} + \frac{3}{8} \end{aligned} \tag{5}$$

their combinations for the thickness functions are

$$\begin{aligned} F_t &= \frac{P_0 + P_1}{2}, \qquad F_b = \frac{P_0 - P_1}{2} \\ F_l &= P_l - P_{l-2} \quad \text{with} \quad l = 2, \ldots, N \end{aligned} \tag{6}$$

The chosen functions have the following interesting properties:

At the top:

$$\zeta_k = 1\text{: } F_t = 1, \qquad F_b = 0, \qquad F_l = 0 \tag{7}$$

At the bottom:

$$\zeta_k = -1\text{: } F_t = 0, \qquad F_b = 1, \qquad F_l = 0 \tag{8}$$

where interface values of the variables are considered as variable unknowns.

The LW model can be conveniently used even though a plate is constituted by only one layer, via the introduction of mathematical interfaces and by using an N order of expansion in the corresponding fictitious layers. Accuracy of the solution can be increased by increasing the number of the mathematical interfaces.

III. Extension of the Unified Formulation to FGM

A model for the analysis of FGM plates must accurately describe the continuous variations of the material characteristics (mechanical, thermal, or electrical) along the thickness. The present section will focus on the procedure that permits extending the UF to the analysis of FGM layers. These layers could be single or embedded in other classical and/or FGM layers. For the FGM layers, we use Legendre polynomials to approximate the elastic coefficients in the thickness z, as done for the LW case in the previous section.

The variation of the material characteristics are usually given in terms of exponential and/or polynomial functions applied directly to the engineering constants such as Young's moduli E_i, shear moduli G_{ij}, and/or Poisson's ratio ν_{ij} or directly to the material stiffnesses $C_{ij}(i, j = 1, 6)$. Actually, because in each point of the plate a relation between the engineering constants and the material stiffnesses holds, only the second case can be treated. Generally, the variation of the stiffness matrix is given by multiplying it by a function of z:

$$\boldsymbol{C}(z) = \boldsymbol{C}_0 * g(z) \tag{9}$$

where $\boldsymbol{C}_0$ is the reference stiffness matrix and $g(z)$ gives the variation along z. By applying the ideas behind the UF, the following expansion is made:

$$\boldsymbol{C}(z) = F_b(z)\boldsymbol{C}_b + F_\gamma(z)\boldsymbol{C}_\gamma + F_t(z)\boldsymbol{C}_t = F_r\boldsymbol{C}_r \tag{10}$$

where the new thickness functions F_γ are the same as the LW expansion in Eq. (4):

$$\begin{aligned} F_t &= \frac{P_0 + P_1}{2}, \qquad F_b = \frac{P_0 - P_1}{2} \\ F_\gamma &= P_\gamma - P_{\gamma-2} \qquad \gamma = 2, \ldots, N_r \end{aligned} \tag{11}$$

where $P_j = P_j(\zeta_k)$ is the Legendre polynomial of jth order defined in the domain $-1 \leq \zeta_k \leq 1$. Figure 7 explains the preceding expansion procedure.

The actual $\boldsymbol{C}$ is then recovered as a weighted summation on the terms $\boldsymbol{C}_r$. The weights are given by the thickness functions F_r. The order of the expansion can be arbitrarily chosen, as for the displacements. Because of the usual complicated laws used for $g(z)$ in the open literature, the expansion in this work was extended to $N_r = 10$ (see Fig. 7). However, when a simple polynomial $g(z)$ is applied, lower values of N_r could be used.

The procedure to include the varying stiffnesses in the model requires computing the $\boldsymbol{C}_r$ matrices. This task can be accomplished solving a simple algebraic system of order N_r for each component C_{ijr}. Thereafter, the actual values of C at N_r different locations along the thickness $(z_1, \ldots, z_{N_r})$ were calculated and the following formula is obtained:

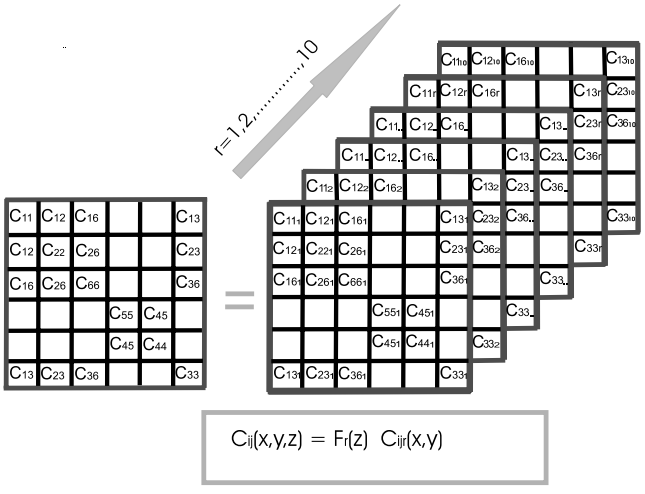

Fig. 7 Expansion scheme for the stiffness matrix $\boldsymbol{C}$.

$$\begin{bmatrix} C_{ij}(z_1) \\ \vdots \\ C_{ij}(z_{N_r}) \end{bmatrix} = \begin{bmatrix} F_b(z_1) & \cdots & F_\gamma(z_1) & \cdots & F_t(z_1) \\ \vdots & & \vdots & & \vdots \\ F_b(z_{N_r}) & \cdots & F_\gamma(z_{N_r}) & \cdots & F_t(z_{N_r}) \end{bmatrix} \begin{bmatrix} C_{ijb} \\ \vdots \\ C_{ijr} \\ \vdots \\ C_{ijt} \end{bmatrix} \tag{12}$$

A. Geometric and Constitutive Relations

Stresses and strains are conveniently grouped into in-plane and normal components, denoted by the subscripts p and n, respectively. Strains of the kth layer can be related to the displacement field $\boldsymbol{u}^k = \{u_x^k, u_y^k, u_z^k\}$ via the geometric relations:

$$\boldsymbol{\epsilon}_p^k = \boldsymbol{D}_p \boldsymbol{u}^k, \qquad \epsilon_n^k = (\boldsymbol{D}_{np} + \boldsymbol{D}_{nz})\boldsymbol{u}^k \tag{13}$$

wherein the differential operator arrays are defined as follows:

$$\boldsymbol{D}_p = \begin{bmatrix} \partial_x & 0 & 0 \\ 0 & \partial_y & 0 \\ \partial_y & \partial_x & 0 \end{bmatrix}, \qquad \boldsymbol{D}_{np} = \begin{bmatrix} 0 & 0 & \partial_x \\ 0 & 0 & \partial_y \\ 0 & 0 & 0 \end{bmatrix}$$
$$\boldsymbol{D}_{nz} = \begin{bmatrix} \partial_z & 0 & 0 \\ 0 & \partial_z & 0 \\ 0 & 0 & \partial_z \end{bmatrix} \tag{14}$$

with $\boldsymbol{\epsilon}_p = (\epsilon_1, \epsilon_2, \epsilon_6) = (\epsilon_{xx}, \epsilon_{yy}, \epsilon_{xy})$ and $\boldsymbol{\epsilon}_n = (\epsilon_5, \epsilon_4, \epsilon_3) = (\epsilon_{xz}, \epsilon_{yz}, \epsilon_{zz})$.

Using the same separation, the expressions of the constitutive relations for a classical plate state:

$$\boldsymbol{\sigma}_p^k = \begin{bmatrix} \sigma_1 \\ \sigma_2 \\ \sigma_6 \end{bmatrix}^k = \begin{bmatrix} C_{11} & C_{12} & C_{16} \\ C_{12} & C_{22} & C_{26} \\ C_{16} & C_{26} & C_{66} \end{bmatrix}^k \begin{bmatrix} \epsilon_1 \\ \epsilon_2 \\ \epsilon_6 \end{bmatrix}^k + \begin{bmatrix} 0 & 0 & C_{13} \\ 0 & 0 & C_{23} \\ 0 & 0 & C_{36} \end{bmatrix}^k \begin{bmatrix} \epsilon_5 \\ \epsilon_4 \\ \epsilon_3 \end{bmatrix}^k = \boldsymbol{C}_{pp}^k \boldsymbol{\epsilon}_p^k + \boldsymbol{C}_{pn}^k \boldsymbol{\epsilon}_n^k \tag{15}$$

$$\boldsymbol{\sigma}_n^k = \begin{bmatrix} \sigma_5 \\ \sigma_4 \\ \sigma_3 \end{bmatrix}^k = \begin{bmatrix} 0 & 0 & 0 \\ 0 & 0 & 0 \\ C_{13} & C_{23} & C_{36} \end{bmatrix}^k \begin{bmatrix} \epsilon_1 \\ \epsilon_2 \\ \epsilon_6 \end{bmatrix}^k + \begin{bmatrix} C_{55} & C_{45} & 0 \\ C_{45} & C_{44} & 0 \\ 0 & 0 & C_{33} \end{bmatrix}^k \begin{bmatrix} \epsilon_5 \\ \epsilon_4 \\ \epsilon_3 \end{bmatrix}^k = \boldsymbol{C}_{pn}^{kT} \boldsymbol{\epsilon}_p^k + \boldsymbol{C}_{nn}^k \boldsymbol{\epsilon}_n^k \tag{16}$$

with $\boldsymbol{\sigma}_p = (\sigma_1, \sigma_2, \sigma_6) = (\sigma_{xx}, \sigma_{yy}, \sigma_{xy})$ and $\boldsymbol{\sigma}_n = (\sigma_5, \sigma_4, \sigma_3) = (\sigma_{xz}, \sigma_{yz}, \sigma_{zz})$, and k is the considered layer.

Thus, taking into account the expansion introduced in Eq. (10) for the stiffnesses matrices, the following expressions can be obtained:

$$\boldsymbol{\sigma}_p = F_r \boldsymbol{C}_{ppr}^k \boldsymbol{\epsilon}_p^k + F_r \boldsymbol{C}_{pnr}^k \boldsymbol{\epsilon}_n^k \tag{17}$$

$$\boldsymbol{\sigma}_n = F_r \boldsymbol{C}_{pnr}^{kT} \boldsymbol{\epsilon}_p^k + F_r \boldsymbol{C}_{nnr}^k \boldsymbol{\epsilon}_n^k \tag{18}$$

These will be used in the derivation of the governing equations for a plate with some FGM layers.

IV. Governing Equations

This section presents the derivation of the governing equations based on the classical principle of virtual displacements (PVD) for FGM plates. Both a closed-form and a finite element solution will be developed. The procedure is finalized to obtain the so-called fundamental nuclei (see [17,18]). These consist of 3×3 arrays that represent the basic items from which the stiffness matrix of the whole structure can be computed.

For a laminate of N_L layers, the principle of virtual displacements for pure mechanical analysis, neglecting any body forces and considering only applied traction loads, is formulated as

$$\sum_{k=1}^{N_L} \int_{\Omega_k} \int_{A_k} \left\{ \delta \boldsymbol{\epsilon}_{pG}^{kT} \boldsymbol{\sigma}_{pC}^k + \delta \boldsymbol{\epsilon}_{nG}^{kT} \boldsymbol{\sigma}_{nC}^k \right\} \mathrm{d}\Omega_k \, \mathrm{d}z = \sum_{k=1}^{N_L} \delta L_e^k \tag{19}$$

where the integration domains Ω_k and A_k indicate, respectively, the reference plane of the lamina and its thickness; subscripts G and C indicate geometrical and constitutive equations, respectively; and δL_e^k is the expression of the external work that takes into account the external loads for a generic layer k. The first step of the procedure to obtain the expression of the fundamental nuclei consists of substituting of the constitutive equations (15) and (16) and the geometrical relations (13) into Eq. (19):

$$\int_{\Omega_k} \int_{A_k} \Big((\boldsymbol{D}_p \delta \boldsymbol{u}^k)^T \Big\{ \Big[\boldsymbol{C}_{pp}^k \boldsymbol{D}_p + \boldsymbol{C}_{pn}^k (\boldsymbol{D}_{np} + \boldsymbol{D}_{nz}) \Big] \boldsymbol{u}^k \Big\} + [(\boldsymbol{D}_{np} + \boldsymbol{D}_{nz}) \delta \boldsymbol{u}^k]^T \Big\{ \Big[\boldsymbol{C}_{pn}^{kT} \boldsymbol{D}_p + \boldsymbol{C}_{nn}^k (\boldsymbol{D}_{np} + \boldsymbol{D}_{nz}) \Big] \boldsymbol{u}^k \Big\} \Big) \mathrm{d}\Omega_k \, \mathrm{d}z = \delta L_e^k \tag{20}$$

By employing the unified formulation for the displacement through Eq. (1) and for the material stiffness matrices via Eq. (10), the previous equation can be rewritten as

$$\int_{\Omega_k} \int_{A_k} \Big(\Big[(\boldsymbol{D}_p) \Big(F_s \delta \boldsymbol{u}_s^k \Big) \Big]^T \Big\{ [F_r \boldsymbol{C}_{ppr}^k \boldsymbol{D}_p + F_r \boldsymbol{C}_{pnr}^k (\boldsymbol{D}_{np} + \boldsymbol{D}_{nz}) \Big] \Big(F_\tau \boldsymbol{u}_\tau^k \Big) \Big\} + \Big[(\boldsymbol{D}_{np} + \boldsymbol{D}_{nz}) \Big(F_s \delta \boldsymbol{u}_s^k \Big) \Big]^T \times \Big\{ \Big[F_r \boldsymbol{C}_{npr}^k \boldsymbol{D}_p + F_r \boldsymbol{C}_{nnr}^k (\boldsymbol{D}_{np} + \boldsymbol{D}_{nz}) \Big] \Big(F_\tau \boldsymbol{u}_\tau^k \Big) \Big\} \Big) \mathrm{d}\Omega_k \, \mathrm{d}z = \delta L_e^k \tag{21}$$

Introducing the following notations

$$(E_{\tau sr}, E_{\tau_{,z} sr}, E_{\tau s_{,z} r}, E_{\tau_{,z} s_{,z} r}) = \int_{A_k} (F_\tau F_s F_r, F_{\tau_{,z}} F_s F_r, F_\tau F_{s_{,z}} F_r, F_{\tau_{,z}} F_{s_{,z}} F_r) \, \mathrm{d}z \tag{22}$$

where z indicates partial derivative respect to z, Eq. (21) can be compacted as

$$\int_{\Omega_k} \Big[\Big(\boldsymbol{D}_p \delta \boldsymbol{u}_s^k \Big)^T \Big(E_{\tau sr} \boldsymbol{C}_{ppr}^k \boldsymbol{D}_p \boldsymbol{u}_\tau^k + E_{\tau sr} \boldsymbol{C}_{pnr}^k \boldsymbol{D}_{np} \boldsymbol{u}_\tau^k + E_{\tau_{,z} sr} \boldsymbol{C}_{pnr}^k \boldsymbol{u}_\tau^k \Big) + \Big(\boldsymbol{D}_{np} \delta \boldsymbol{u}_s^k \Big)^T \Big(E_{\tau sr} \boldsymbol{C}_{npr}^k \boldsymbol{D}_p \boldsymbol{u}_\tau^k + E_{\tau sr} \boldsymbol{C}_{nnr}^k \boldsymbol{D}_{np} \boldsymbol{u}_\tau^k + E_{\tau_{,z} sr} \boldsymbol{C}_{nnr}^k \boldsymbol{u}_\tau^k \Big) + \Big(\delta \boldsymbol{u}_s^k \Big)^T \Big(E_{\tau s_{,z} r} \boldsymbol{C}_{npr}^k \boldsymbol{D}_p \boldsymbol{u}_\tau^k + E_{\tau s_{,z} r} \boldsymbol{C}_{nnr}^k \boldsymbol{D}_{np} \boldsymbol{u}_\tau^k + E_{\tau_{,z} s_{,z} r} \boldsymbol{C}_{nnr}^k \boldsymbol{u}_\tau^k \Big) \Big] \mathrm{d}\Omega_k = \delta L_e^k \tag{23}$$

Closed-form and finite element governing equations are derived in the next two subsections; also see [18,19] for details on the used techniques.

A. Fundamental Nuclei for the Governing Differential Equations

The integration by parts is requested to obtain a strong form of differential equations on the domain Ω_k and boundary conditions on

edge Γ_k. For a generic variable $\boldsymbol{a}^k$, the integration by parts states:

$$\int_{\Omega_k} [(\boldsymbol{D}_\Omega)\delta\boldsymbol{a}^k]^T \boldsymbol{a}^k \, \mathrm{d}\Omega_k = -\int_{\Omega_k} \delta\boldsymbol{a}^{kT}\left[\left(\boldsymbol{D}_\Omega^T\right)\boldsymbol{a}^k\right]\mathrm{d}\Omega_k + \int_{\Gamma_k} \delta\boldsymbol{a}^{kT}[(\boldsymbol{I}_\Omega)\boldsymbol{a}^k]\,\mathrm{d}\Gamma_k \tag{24}$$

where $\Omega = p, np$.

The governing equations are

$$\delta\boldsymbol{u}_s^{kT}: \boldsymbol{K}_{uu}^{k\tau sr}\boldsymbol{u}_\tau^k = \boldsymbol{P}_{u\tau}^k \tag{25}$$

and the boundary conditions state

$$\boldsymbol{\Pi}_{uu}^{k\tau sr}\boldsymbol{u}_\tau^k = \boldsymbol{\Pi}_{uu}^{k\tau sr}\bar{\boldsymbol{u}}_\tau^k \tag{26}$$

In Eq. (25), $\boldsymbol{P}_{u\tau}^k$ is the external load, and the fundamental nucleus $\boldsymbol{K}_{uu}^{k\tau sr}$ has to be assembled through the depicted indexes: the internal loop is on index r; τ and s consider the order of expansion in z for the displacements; and superscript k denotes the assembling on the number of layers. The governing equations of FGM plates discussed in Figs. 2 and 3 are formally the same as those obtained for the classical multilayer plate [19], the only difference is the index r.

The explicit form of the fundamental nuclei are

$$\begin{aligned}\boldsymbol{K}_{uu}^{k\tau sr} = \Big\{&\left(-\boldsymbol{D}_p^T\right)\left[\boldsymbol{C}_{ppr}^k E_{\tau sr}\boldsymbol{D}_p + \boldsymbol{C}_{pnr}^k E_{\tau sr}\boldsymbol{D}_{np} + \boldsymbol{C}_{pnr}^k E_{\tau_{,z}sr}\right] \\ &- \left(\boldsymbol{D}_{np}^T\right)\left[\boldsymbol{C}_{pnr}^k E_{\tau sr}\boldsymbol{D}_p + \boldsymbol{C}_{nnr}^k E_{\tau sr}\boldsymbol{D}_{np} + \boldsymbol{C}_{nnr}^k E_{\tau_{,z}sr}\right] \\ &+ \left[\boldsymbol{C}_{npr}^k E_{\tau s_{,z}r}\boldsymbol{D}_p + \boldsymbol{C}_{nnr}^k E_{\tau s_{,z}r}\boldsymbol{D}_{np} + \boldsymbol{C}_{nnr}^k E_{\tau_{,z}s_{,z}r}\right]\Big\}\end{aligned} \tag{27}$$

and for the boundary conditions,

$$\begin{aligned}\boldsymbol{\Pi}_{uu}^{k\tau sr} = \Big\{&(\boldsymbol{I}_p)\left[\boldsymbol{C}_{ppr}^k E_{\tau sr}\boldsymbol{D}_p + \boldsymbol{C}_{pnr}^k E_{\tau sr}\boldsymbol{D}_{np} + \boldsymbol{C}_{pnr}^k E_{\tau_{,z}sr}\right] \\ &+ (\boldsymbol{I}_{np})\left[\boldsymbol{C}_{pnr}^k E_{\tau sr}\boldsymbol{D}_p + \boldsymbol{C}_{nnr}^k E_{\tau sr}\boldsymbol{D}_{np} + \boldsymbol{C}_{nnr}^k E_{\tau_{,z}sr}\right]\Big\}\end{aligned} \tag{28}$$

The following additional arrays were introduced to perform integration by parts:

$$\boldsymbol{I}_p = \begin{bmatrix}1 & 0 & 0\\ 0 & 1 & 0\\ 1 & 1 & 0\end{bmatrix}, \qquad \boldsymbol{I}_{np} = \begin{bmatrix}0 & 0 & 1\\ 0 & 0 & 1\\ 0 & 0 & 0\end{bmatrix} \tag{29}$$

Closed-form solutions of the Navier type are possible for simply supported plates and transversely isotropic materials. Transversely isotropic materials means that

$$C_{pp16} = C_{pp26} = C_{pn63} = C_{pn36} = C_{nn45} = 0$$

The following harmonic assumptions can be made for the field variables:

$$\begin{aligned}u_{x_\tau}^k &= \sum_{m,n}\left(\hat{U}_{x_\tau}^k\right)\cos\frac{m\pi x_k}{a_k}\sin\frac{n\pi y_k}{b_k} && k = 1, N_l\\ u_{y_\tau}^k &= \sum_{m,n}\left(\hat{U}_{y_\tau}^k\right)\sin\frac{m\pi x_k}{a_k}\cos\frac{n\pi y_k}{b_k} && \tau = t, b, r\\ u_{z_\tau}^k &= \sum_{m,n}\left(\hat{U}_{z_\tau}^k\right)\sin\frac{m\pi x_k}{a_k}\sin\frac{n\pi y_k}{b_k} && r = 2, N\end{aligned} \tag{30}$$

where $\hat{U}_{x_\tau}^k$, $\hat{U}_{y_\tau}^k$, and $\hat{U}_{z_\tau}^k$ are the amplitudes; m and n are the number of waves (they go from zero to infinite, as illustrated in [26,27]); and a_k and b_k are the dimensions of the plate. The governing equations in Eq. (25) become a system of algebraic equations. The explicit form of the fundamental nuclei is given in the Appendix.

B. Fundamental Nuclei for the Finite Element Solution

In the finite element method, the unknowns are expressed in terms of their nodal values, via the shape functions N_j:

$$\boldsymbol{u}_\tau^k(x, y) = \boldsymbol{N}_j\boldsymbol{q}_{\tau j}^k \qquad j = 1, 2, \ldots, N_n \tag{31}$$

where N_n denotes the number of nodes of the element, and

$$\boldsymbol{q}_{\tau j}^k = \begin{bmatrix}q_{u_x\tau j}^k\\ q_{u_y\tau j}^k\\ q_{u_z\tau j}^k\end{bmatrix} \tag{32}$$

Substituting Eq. (31) in Eq. (1), the final expression of the displacement field can be obtained:

$$\boldsymbol{u}^k(x, y, z) = F_\tau\boldsymbol{N}_j\boldsymbol{q}_{\tau j}^k, \qquad \delta\boldsymbol{u}^k(x, y, z) = F_s\boldsymbol{N}_i\delta\boldsymbol{q}_{si}^k \tag{33}$$

Introducing the discretized expression of the displacement field into the internal work equation (23), it assumes the following expression:

$$\begin{aligned}\delta L_i^k = \int_{\Omega_k} \Big\{&\left(\delta\boldsymbol{q}_{si}^k\right)^T[\boldsymbol{D}_p\boldsymbol{N}_i]^T\Big[\Big(E_{\tau sr}\boldsymbol{C}_{ppr}^k(\boldsymbol{D}_p\boldsymbol{N}_j) \\ &+ E_{\tau sr}\boldsymbol{C}_{pnr}^k(\boldsymbol{D}_{np}\boldsymbol{N}_j) + E_{\tau_{,z}sr}\boldsymbol{C}_{pnr}^k\boldsymbol{N}_j\boldsymbol{I}\Big)\boldsymbol{q}_{\tau j}^k\Big] \\ &+ \left(\delta\boldsymbol{q}_{si}^k\right)^T[\boldsymbol{D}_{np}\boldsymbol{N}_i]^T\Big[\Big(E_{\tau sr}\boldsymbol{C}_{npr}^k(\boldsymbol{D}_p\boldsymbol{N}_j) + E_{\tau sr}\boldsymbol{C}_{nnr}^k(\boldsymbol{D}_{np}\boldsymbol{N}_j) \\ &+ E_{\tau_{,z}sr}\boldsymbol{C}_{nnr}^k\boldsymbol{N}_j\boldsymbol{I}\Big)\boldsymbol{q}_{\tau j}^k\Big] + \left(\delta\boldsymbol{q}_{si}^k\right)^T[\boldsymbol{N}_i\boldsymbol{I}]^T\Big[(E_{\tau s_{,z}r}\boldsymbol{C}_{npr}^k(\boldsymbol{D}_p\boldsymbol{N}_j) \\ &+ E_{\tau s_{,z}r}\boldsymbol{C}_{nnr}^k(\boldsymbol{D}_{np}\boldsymbol{N}_j) + E_{\tau_{,z}s_{,z}r}\boldsymbol{C}_{nnr}^k\boldsymbol{N}_j\boldsymbol{I}\Big)\boldsymbol{q}_{\tau j}^k\Big]\Big\}\,\mathrm{d}\Omega_k \\ &= \delta\boldsymbol{q}_{si}^{kT}\boldsymbol{K}_{uu}^{k\tau srij}\boldsymbol{p}_{\tau j}\end{aligned} \tag{34}$$

where $\boldsymbol{I}$ is the unit array.

By conveniently regrouping the terms of Eq. (34), the following term can be easily obtained:

$$\begin{aligned}\boldsymbol{K}_{uu}^{k\tau srij} = \int_{\Omega_k} \Big\{&\left(\boldsymbol{D}_p^T\boldsymbol{N}_i\right)\Big[\boldsymbol{C}_{ppr}^k E_{\tau sr}(\boldsymbol{D}_p\boldsymbol{N}_j) + \boldsymbol{C}_{pnr}^k E_{\tau sr}(\boldsymbol{D}_{np}\boldsymbol{N}_j) \\ &+ \boldsymbol{C}_{pnr}^k E_{\tau_{,z}sr}(\boldsymbol{N}_j\boldsymbol{I})\Big] + \left(\boldsymbol{D}_{np}^T\boldsymbol{N}_i\right)\Big[\boldsymbol{C}_{npr}^k E_{\tau sr}(\boldsymbol{D}_p\boldsymbol{N}_j) \\ &+ \boldsymbol{C}_{nnr}^k E_{\tau sr}(\boldsymbol{D}_{np}\boldsymbol{N}_j) + \boldsymbol{C}_{nnr}^k E_{\tau_{,z}sr}(\boldsymbol{N}_j\boldsymbol{I})\Big] \\ &+ (\boldsymbol{N}_i\boldsymbol{I})\Big[\boldsymbol{C}_{npr}^k E_{\tau s_{,z}r}(\boldsymbol{D}_p\boldsymbol{N}_j) + \boldsymbol{C}_{nnr}^k E_{\tau s_{,z}r}(\boldsymbol{D}_{np}\boldsymbol{N}_j) \\ &+ \boldsymbol{C}_{nnr}^k E_{\tau_{,z}s_{,z}r}(\boldsymbol{N}_j\boldsymbol{I})\Big]\Big\}\,\mathrm{d}\Omega_k\end{aligned} \tag{35}$$

The same procedure can be applied to the external work done by forces. Because the procedure does not present any differences from the classical material cases, it is not reported here. The complete derivation can be found in [19]. The final expression for the external work reads:

$$\delta L_e^k = \delta\boldsymbol{q}_{si}^{kT}\boldsymbol{K}_{up}^{k\tau srij}\boldsymbol{p}_{\tau j} = \delta\boldsymbol{q}_{si}^{kT}\boldsymbol{P}_{u\tau}^k \tag{36}$$

where $\boldsymbol{p}_{\tau j}^k$ contains the load nodal amplitudes. The PVD leads to

$$\delta\boldsymbol{q}_{si}^{kT}: \boldsymbol{K}_{uu}^{k\tau srij}\boldsymbol{q}_{\tau j}^k = \boldsymbol{P}_{u\tau}^k \tag{37}$$

the nucleus $\boldsymbol{K}_{uu}^{k\tau srij}$ has two additional indexes with respect to the nuclei for the closed-form solution: i and j are related to shape functions and to nodes of the considered FE. The explicit expression of the fundamental nuclei is given in the Appendix.

V. Compared Theories

The FGM plates considered in this paper are only constituted by one FGM layer. The ESL model could be sufficient for these plates. The index r of Eq. (10) is always set to the value 10, and the expansion for displacements ranges from $N = 1$ (linear) to $N = 4$ (fourth order). The FSDT is a particular case of the $N = 1$ theory when the transversal displacement is constant ($u_z = u_{z0}$).

Mathematical interlayers are introduced in the case of the problem considered by Zenkour [3] to provide a reference solution: this is a CF solution obtained via a layerwise model ($N = 4$) applied to 100 mathematical layers (constant properties for each layer); this solution will be indicated with $N_{\text{ml}} = 100$ (CF). A numerical assessment not documented in this paper has shown that 100 mathematical layers leads to a 3D description of stresses and displacements for FGM plates.

VI. Numerical Results

The two problems considered in [2,3], which are related to a simply supported FGM rectangular plate subjected to a transversal mechanical load, have been addressed to assess the capabilities of the proposed formulation. The results are given for the FE and CF solutions in the form of tables and graphs. The finite element model uses a nine-node element with a 6×6 mesh for which a convergent solution was reached.

A. Case 1

The three-dimensional solution presented in [2] considers a square plate of global thickness h and side-to-thickness ratio $a/h = 3$, which is subjected to a transverse bisinusoidal ($m = n = 1$) loading of amplitude q applied to its top surface. The shear modulus is assumed to vary exponentially through the thickness (Poisson's ratio is considered to be constant) according to

$$G(z) = G_1 e^{\gamma(z/h-1)}, \qquad G_1 = \frac{E_1}{2(1+\nu)} \qquad 0 \le z \le h \tag{38}$$

The normalized out-of-plane displacement u_z is reported in Table 1 at the midsurface of the plate for different values of inhomogeneity parameter γ. The closed-form and finite element solutions are both in agreement with the 3D solution proposed by Kashtalyan [2], and 3D solutions are obtained in the $N = 4$ cases for the considered very thick plate ($a/h = 3$). It could be concluded that the presented implementation works well and the UF is able to give a 3D description of FGM plates. The FE solutions completely agree with the correspondent CF cases; therefore, the accuracy of the used 6×6 mesh is confirmed.

B. Case 2

The generalized shear deformation model proposed in [3] was applied to a square plate with a global thickness of 0.1 m and a side-to-thickness ratio $a/h = 10$, subjected to a transversal bisinusoidal loading ($m = n = 1$) of amplitude $q_0 = 1.0$ Pa applied to its top surface. The plate is made of aluminum (bottom) and alumina (top), and the following functional relationship is considered for $E(z)$:

$$E(z) = E_m + (E_c - E_m)\left(\frac{2z+h}{2h}\right)^{\kappa} \qquad -\frac{h}{2} \le z \le \frac{h}{2} \tag{39}$$

where $E_m = 70$ GPa and $E_c = 380$ GPa are the corresponding properties of the metal and ceramic, respectively, and κ is the volume fraction exponent that takes values greater than or equal to zero. Poisson's ratio is considered to be constant and equal to 0.3. The results are given in terms of the following nondimensional parameters:

$$\bar{u} = \frac{100h^3E_c}{a^4q_0}u_x\left(0, \frac{b}{2}, -\frac{h}{4}\right), \qquad \bar{v} = \frac{10h^3E_c}{a^4q_0}u_y\left(\frac{a}{2}, 0, -\frac{h}{6}\right)$$

$$\bar{w} = \frac{10h^3E_c}{a^4q_0}u_z\left(\frac{a}{2}, \frac{b}{2}, 0\right), \qquad \bar{\sigma}_{yy} = \frac{h}{aq_0}\sigma_{yy}\left(\frac{a}{2}, \frac{b}{2}, \frac{h}{3}\right)$$

$$\bar{\sigma}_{xy} = \frac{h}{aq_0}\sigma_{xy}\left(0, 0, -\frac{h}{3}\right), \qquad \bar{\sigma}_{yz} = \frac{h}{aq_0}\sigma_{yz}\left(\frac{a}{2}, 0, \frac{h}{6}\right)$$

$$\bar{\sigma}_{zz} = \frac{h}{aq_0}\sigma_{zz}$$

The results are given in Tables 2 and 3 for different values of exponential κ. The results are given in Table 2 for values of κ that go from 1 to 10. The reference solution is given in [3], which considers transversal displacement u_z to be constant. An alternative reference solution was introduced to confirm the superiority of the present model with respect to solution [3], which makes use of mathematical interfaces (see Sec. V); a layerwise model ($N = 4$) is employed by considering the plate to be divided into 100 mathematical layers, in which each single layer has constant elastic properties [this is denoted as $N_{\text{ml}} = 100$ (CF)]; due to computation-time costs, attention has been restricted to the CF case.

The stresses are reported in Table 3. Closed-form solutions are, of course, more efficient than FE solutions. The CF and $N_{\text{ml}} = 100$ (CF) cases show the improvements with respect to the analysis in [3]. Furthermore, the present advanced models permit very good results to be obtained for out-of-plane variables and stresses.

Figures 8 and 9 show that in-plane stress σ_{yy} related to the ESL analysis is very close to the $N_{\text{ml}} = 100$ (CF) solution but some difficulties are exhibited for normal stress σ_{zz} evaluation; in particular, the top and bottom stress conditions are not completely satisfied. The extension of Reissner's [28] mixed variational theorem could be a remedy to this problem.

VII. Conclusions

The extension of UF to FGM plates was provided in this paper. A variable kinematic model was obtained that permits different plate cases to be considered in a unified manner, in which various material laws through the thickness are given. The method is very general and

Table 1 Case 1 normalized out-of-plane displacement $(G_1u_z/qh)/[(a/2), (b/2), (h/2)]$ in a functionally graded plate and a homogeneous plate.

		Closed form				Finite element	
γ	3D[a]	$N = 4$	$N = 2$	$N = 1$	FSDT	$N = 4$	$N = 3$
10^{-1}	−1.4146	−1.4145	−1.3480	−1.2271	−1.2285	−1.4148	−1.4167
10^{-2}	−1.3496	−1.3495	−1.2856	−1.1744	−1.1746	−1.3497	−1.3516
10^{-3}	−1.3433	−1.3431	−1.2796	−1.1693	−1.1693	−1.3434	−1.3453
10^{-4}	−1.3426	−1.3425	−1.2789	−1.1688	−1.1688	−1.3427	−1.3446
10^{-5}	−1.3426	−1.3424	−1.2789	−1.1687	−1.1687	−1.3427	−1.3446
10^{-6}	−1.3426	−1.3424	−1.2789	−1.1687	−1.1687	−1.3427	−1.3446
-10^{-1}	−1.2740	−1.2739	−1.2132	−1.1129	−1.1116	−1.2741	−1.2759
-10^{-2}	−1.3355	−1.3354	−1.2722	−1.1630	−1.1629	−1.3357	−1.3375
-10^{-3}	−1.3419	−1.3417	−1.2782	−1.1681	−1.1681	−1.3420	−1.3439
-10^{-4}	−1.3425	−1.3424	−1.2788	−1.1686	−1.1686	−1.3426	−1.3445
-10^{-5}	−1.3425	−1.3424	−1.2789	−1.1687	−1.1687	−1.3427	−1.3445
-10^{-6}	−1.3425	−1.3424	−1.2789	−1.1687	−1.1687	−1.3427	−1.3446
0	−1.3430	−1.3424	−1.2789	−1.1687	−1.1687	−1.3427	−1.3445

[a]Three-dimensional solutions are by Kashtalyan [2].

Table 2 Case 2 results for displacements of the $N = 4$ model for the CF and FE solutions.[a]

κ	Model	$\bar{u}$	$\bar{v}$	$\bar{w}$
	Reference	0.6626	0.5093	0.5889
	$N_{ml} = 100$ (CF)	0.6436	0.4970	0.5875
	$N = 4$ (CF)	0.6435	0.4981	0.5875
1	$N = 4$ (FE)	0.6438	0.4982	0.5876
	Reference	0.9281	0.7311	0.7573
	$N_{ml} = 100$ (CF)	0.9012	0.7149	0.7570
	$N = 4$ (CF)	0.9012	0.7162	0.7570
2	$N = 4$ (FE)	0.9016	0.7164	0.7571
	Reference	1.0447	0.8271	0.8377
	$N_{ml} = 100$ (CF)	1.0106	0.8065	0.8381
	$N = 4$ (CF)	1.0111	0.8086	0.8381
3	$N = 4$ (FE)	1.0115	0.8089	0.8383
	Reference	1.0941	0.8651	0.8819
	$N_{ml} = 100$ (CF)	1.0541	0.8401	0.8823
	$N = 4$ (CF)	1.0548	0.8430	0.8822
4	$N = 4$ (FE)	1.0553	0.8433	0.8823
	Reference	1.1158	0.8792	0.9118
	$N_{ml} = 100$ (CF)	1.0716	0.8506	0.9118
	$N = 4$ (CF)	1.0724	0.8540	0.9116
5	$N = 4$ (FE)	1.0728	0.8543	0.9118
	Reference	1.1261	0.8834	0.9356
	$N_{ml} = 100$ (CF)	1.0788	0.8519	0.9351
	$N = 4$ (CF)	1.0794	0.8554	0.9349
6	$N = 4$ (FE)	1.0798	0.8557	0.9350
	Reference	1.1312	0.8832	0.9562
	$N_{ml} = 100$ (CF)	1.0817	0.8497	0.9554
	$N = 4$ (CF)	1.0821	0.8530	0.9551
7	$N = 4$ (FE)	1.0826	0.8533	0.9552
	Reference	1.1340	0.8813	0.9750
	$N_{ml} = 100$ (CF)	1.0830	0.8462	0.9738
	$N = 4$ (CF)	1.0832	0.8492	0.9735
8	$N = 4$ (FE)	1.0837	0.8495	0.9737
	Reference	1.1358	0.8785	0.9925
	$N_{ml} = 100$ (CF)	1.0837	0.8424	0.9911
	$N = 4$ (CF)	1.0837	0.8451	0.9908
9	$N = 4$ (FE)	1.0841	0.8454	0.9910
	Reference	1.1372	0.8756	1.0089
	$N_{ml} = 100$ (CF)	1.0842	0.8387	1.0074
	$N = 4$ (CF)	1.0841	0.8411	1.0072
10	$N = 4$ (FE)	1.0845	0.8414	1.0074

[a]Mathematical interfaces and the corresponding layerwise solution ($N = 4$ for each layer with constant elastic properties) are obtained in CF, dividing the plate in 100 homogeneous mathematical layers ($N_{ml} = 100$). The reference solution is by Zenkour [3]

Table 3 Case 2 results for stresses of the $N = 4$ model for the CF and FE solutions.[a]

κ	Model	$\bar{\sigma}_{yy}$	$\bar{\sigma}_{yz}$	$\bar{\sigma}_{xy}$
	Reference	1.4894	0.2622	0.6110
	$N_{ml} = 100$ (CF)	1.5062	0.2510	0.6081
	$N = 4$ (CF)	1.5064	0.2509	0.6112
1	$N = 4$ (FE)	1.5411	0.3631	0.6244
	Reference	1.3954	0.2763	0.5441
	$N_{ml} = 100$ (CF)	1.4147	0.2496	0.5421
	$N = 4$ (CF)	1.4139	0.2516	0.5437
2	$N = 4$ (FE)	1.4463	0.3601	0.5555
	Reference	1.2748	0.2715	0.5525
	$N_{ml} = 100$ (CF)	1.2948	0.2420	0.5515
	$N = 4$ (CF)	1.2936	0.2450	0.5522
3	$N = 4$ (FE)	1.3231	0.3386	0.5641
	Reference	1.1783	0.2580	0.5667
	$N_{ml} = 100$ (CF)	1.1985	0.2362	0.5666
	$N = 4$ (CF)	1.1971	0.2361	0.5670
4	$N = 4$ (FE)	1.2244	0.3160	0.5792
	Ref.	1.1029	0.2429	0.5755
	$N_{ml} = 100$ (CF)	1.1233	0.2324	0.5761
	$N = 4$ (CF)	1.1219	0.2271	0.5763
5	$N = 4$ (FE)	1.1474	0.2968	0.5887
	Reference	1.0417	0.2296	0.5803
	$N_{ml} = 100$ (CF)	1.0625	0.2297	0.5817
	$N = 4$ (CF)	1.0609	0.2198	0.5817
6	$N = 4$ (FE)	1.0849	0.2825	0.5943
	Reference	0.9903	0.2194	0.5834
	$N_{ml} = 100$ (CF)	1.0117	0.2277	0.5852
	$N = 4$ (CF)	1.0097	0.2147	0.5853
7	$N = 4$ (FE)	1.0326	0.2728	0.5979
	Reference	0.9466	0.2121	0.5856
	$N_{ml} = 100$ (CF)	0.9687	0.2262	0.5879
	$N = 4$ (CF)	0.9660	0.2118	0.5880
8	$N = 4$ (FE)	0.9879	0.2670	0.6007
	Reference	0.9092	0.2072	0.5875
	$N_{ml} = 100$ (CF)	0.9320	0.2249	0.5902
	$N = 4$ (CF)	0.9286	0.2107	0.5903
9	$N = 4$ (FE)	0.9496	0.2640	0.6030
	Reference	0.8775	0.2041	0.5894
	$N_{ml} = 100$ (CF)	0.9009	0.2237	0.5923
	$N = 4$ (CF)	0.8967	0.2108	0.5925
10	$N = 4$ (FE)	0.9171	0.2632	0.6053

[a]Mathematical interfaces and the corresponding layerwise solution ($N = 4$ for each layer with constant elastic properties) are obtained in CF, dividing the plate in 100 homogeneous mathematical layers ($N_{ml} = 100$). The reference solution is by Zenkour [3]

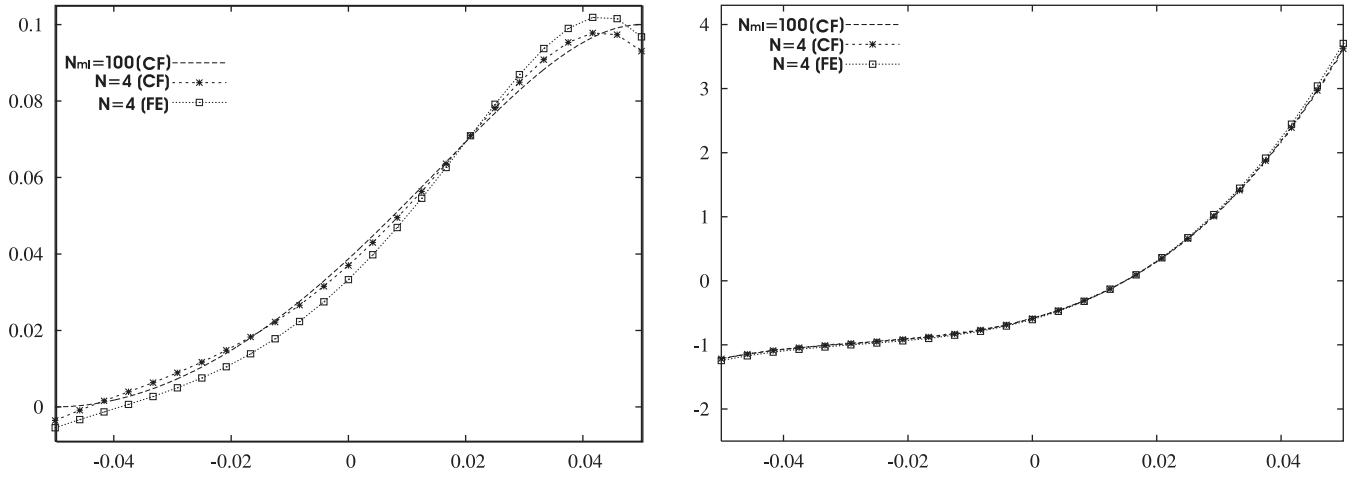

Fig. 8 Case 2 evaluation of normal stress σ_{zz} (left) and in-plane stress σ_{yy} (right) through the thickness z ($\kappa = 2$); comparison between $N = 4$ (CF), $N = 4$ (FE), and the layerwise solution ($N = 4$) applied to 100 mathematical interfaces ($N_{ml} = 100$) in closed form.

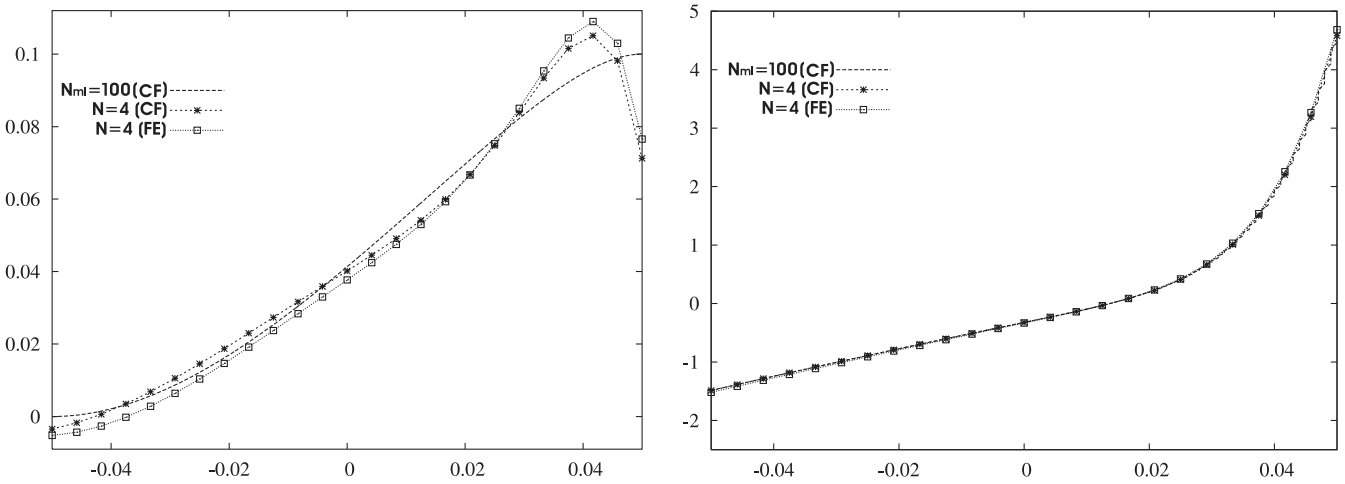

Fig. 9 Case 2 evaluation of normal stress σ_{zz} (left) and in-plane stress σ_{yy} (right) through the thickness z ($\kappa = 7$). Comparison between $N = 4$ (CF), $N = 4$ (FE), and the layerwise solution $N = 4$ applied to 100 mathematical interfaces ($N_{ml} = 100$) in closed form.

the material properties can change with continuity. A comparison with 3D results confirmed the efficiency of the extension of UF to FGM plate analysis. Improvements with respect to classical theories are clearly shown. Additional benchmarks related to FGM/classical multilayer plates could be provided in future works. Future research should also consider the use of Reissner's mixed variational theorem to obtain transverse and normal stresses a priori, as well as the extension to shell geometries and to multifield problems.

Appendix: Fundamental Nuclei

The explicit expressions of the fundamental nuclei are listed next. For closed form, $\alpha = m\pi/a$ and $\beta = n\pi/b$, where m and n are the wave numbers in the in-plane directions, and a and b are the plate dimensions. In the finite element nucleus, the symbol $\lhd \ldots \rhd_{\Omega_k}$ indicates integration over the element domain.

The closed-form nucleus:

$$
\begin{aligned}
K_{uu_{11}} &= C_{55r}E_{\tau_{,z}s_{,z}r} + C_{11r}\alpha^2 E_{\tau sr} + C_{66r}\beta^2 E_{\tau sr}\\
K_{uu_{12}} &= C_{12r}\alpha\beta E_{\tau sr} + C_{66r}\alpha\beta E_{\tau sr}\\
K_{uu_{13}} &= -C_{13r}\alpha E_{\tau_{,z}sr} + C_{55r}\alpha E_{\tau s_{,z}r} \qquad K_{uu_{21}} = K_{uu_{12}}\\
K_{uu_{22}} &= C_{44r}E_{\tau_{,z}s_{,z}r} + C_{22r}\beta^2 E_{\tau sr} + C_{66r}\alpha^2 E_{\tau sr}\\
K_{uu_{23}} &= -C_{23r}\beta E_{\tau_{,z}sr} + C_{44r}\beta E_{\tau s_{,z}r}\\
K_{uu_{31}} &= C_{55r}\alpha E_{\tau_{,z}sr} - C_{13r}\alpha E_{\tau s_{,z}r}\\
K_{uu_{32}} &= C_{44r}\beta E_{\tau_{,z}sr} - C_{23r}\beta E_{\tau s_{,z}r}\\
K_{uu_{33}} &= C_{33r}E_{\tau_{,z}s_{,z}r} + C_{44r}\beta^2 E_{\tau sr} + C_{55r}\alpha^2 E_{\tau sr}
\end{aligned}
$$

The finite element nucleus:

$$
\begin{aligned}
K_{uu_{11}} &= C_{55r}\lhd N_i N_j \rhd_{\Omega_k} E_{\tau_{,z}s_{,z}r} + C_{11r}\lhd N_{i,x} N_{j,x} \rhd_{\Omega_k} E_{\tau sr}\\
&\quad + C_{16r}\lhd N_{i,x} N_{j,y} \rhd_{\Omega_k} E_{\tau sr} + C_{16r}\lhd N_{i,y} N_{j,x} \rhd_{\Omega_k} E_{\tau sr}\\
&\quad + C_{66r}\lhd N_{i,y} N_{j,y} \rhd_{\Omega_k} E_{\tau sr}\\
K_{uu_{12}} &= C_{45r}\lhd N_i N_j \rhd_{\Omega_k} E_{\tau_{,z}s_{,z}r} + C_{16r}\lhd N_{i,x} N_{j,x} \rhd_{\Omega_k} E_{\tau sr}\\
&\quad + C_{12r}\lhd N_{i,x} N_{j,y} \rhd_{\Omega_k} E_{\tau sr} + C_{66r}\lhd N_{i,y} N_{j,x} \rhd_{\Omega_k} E_{\tau sr}\\
&\quad + C_{26r}\lhd N_{i,y} N_{j,y} \rhd_{\Omega_k} E_{\tau sr}\\
K_{uu_{13}} &= C_{13r}\lhd N_{i,x} N_j \rhd_{\Omega_k} E_{\tau_{,z}sr} + C_{36r}\lhd N_{i,y} N_j \rhd_{\Omega_k} E_{\tau s_{,z}r}\\
&\quad + C_{55r}\lhd N_i N_{j,x} \rhd_{\Omega_k} E_{\tau s_{,z}r} + C_{45r}\lhd N_i N_{j,y} \rhd_{\Omega_k} E_{\tau_{,z}sr}
\end{aligned}
$$

$$
\begin{aligned}
K_{uu_{21}} &= C_{45r}\lhd N_i N_j \rhd_{\Omega_k} E_{\tau_{,z}s_{,z}r} + C_{12r}\lhd N_{i,y} N_{j,x} \rhd_{\Omega_k} E_{\tau sr}\\
&\quad + C_{26r}\lhd N_{i,y} N_{j,y} \rhd_{\Omega_k} E_{\tau sr} + C_{16r}\lhd N_{i,x} N_{j,x} \rhd_{\Omega_k} E_{\tau sr}\\
&\quad + C_{66r}\lhd N_{i,x} N_{j,y} \rhd_{\Omega_k} E_{\tau sr}\\
K_{uu_{22}} &= C_{44r}\lhd N_i N_j \rhd_{\Omega_k} E_{\tau_{,z}s_{,z}r} + C_{26r}\lhd N_{i,y} N_{j,x} \rhd_{\Omega_k} E_{\tau sr}\\
&\quad + C_{22r}\lhd N_{i,y} N_{j,y} \rhd_{\Omega_k} E_{\tau sr} + C_{66r}\lhd N_{i,x} N_{j,x} \rhd_{\Omega_k} E_{\tau sr}\\
&\quad + C_{26r}\lhd N_{i,x} N_{j,y} \rhd_{\Omega_k} E_{\tau sr}\\
K_{uu_{23}} &= C_{36r}\lhd N_{i,x} N_j \rhd_{\Omega_k} E_{\tau_{,z}sr} + C_{23r}\lhd N_{i,y} N_j \rhd_{\Omega_k} E_{\tau_{,z}sr}\\
&\quad + C_{45r}\lhd N_i N_{j,x} \rhd_{\Omega_k} E_{\tau s_{,z}r} + C_{44r}\lhd N_i N_{j,y} \rhd_{\Omega_k} E_{\tau s_{,z}r}\\
K_{uu_{31}} &= C_{55r}\lhd N_{i,x} N_j \rhd_{\Omega_k} E_{\tau_{,z}sr} + C_{45r}\lhd N_{i,y} N_j \rhd_{\Omega_k} E_{\tau s_{,z}r}\\
&\quad + C_{13r}\lhd N_i N_{j,x} \rhd_{\Omega_k} E_{\tau s_{,z}r} + C_{36r}\lhd N_i N_{j,y} \rhd_{\Omega_k} E_{\tau_{,z}sr}\\
K_{uu_{32}} &= C_{45r}\lhd N_{i,x} N_j \rhd_{\Omega_k} E_{\tau s_{,z}r} + C_{44r}\lhd N_{i,y} N_j \rhd_{\Omega_k} E_{\tau_{,z}sr}\\
&\quad + C_{36r}\lhd N_i N_{j,x} \rhd_{\Omega_k} E_{\tau_{,z}sr} + C_{23r}\lhd N_i N_{j,y} \rhd_{\Omega_k} E_{\tau s_{,z}r}\\
K_{uu_{33}} &= C_{33r}\lhd N_i N_j \rhd_{\Omega_k} E_{\tau_{,z}s_{,z}r} + C_{45r}\lhd N_{i,y} N_{j,x} \rhd_{\Omega_k} E_{\tau sr}\\
&\quad + C_{44r}\lhd N_{i,y} N_{j,y} \rhd_{\Omega_k} E_{\tau sr} + C_{55r}\lhd N_{i,x} N_{j,x} \rhd_{\Omega_k} E_{\tau sr}\\
&\quad + C_{45r}\lhd N_{i,x} N_{j,y} \rhd_{\Omega_k} E_{\tau sr}
\end{aligned}
$$

References

[1] Reddy, J. N., "Analysis of Functionally Graded Plates," *International Journal for Numerical Methods in Engineering*, Vol. 47, Nos. 1–3, 2000, pp. 663–684. doi:10.1002/(SICI)1097-0207(20000110/30)47:1/3<663::AID-NME787>3.0.CO;2-8

[2] Kashtalyan, M., "Three-Dimensional Elasticity Solution for Bending of Functionally Graded Rectangular Plates," *European Journal of Mechanics, A/Solids*, Vol. 23, No. 5, 2004, pp. 853–864. doi:10.1016/j.euromechsol.2004.04.002

[3] Zenkour, A. M., "Generalized Shear Deformation Theory for Bending Analysis of Functionally Graded Plates," *Applied Mathematical Modelling*, Vol. 30, No. 1, 2006, pp. 67–84. doi:10.1016/j.apm.2005.03.009

[4] Batra, R. C., and Jin, J., "Natural Frequencies of a Functionally Graded Anisotropic Rectangular Plate," *Journal of Sound and Vibration*, Vol. 282, Nos. 1–2, 2005, pp. 509–516. doi:10.1016/j.jsv.2004.03.068

[5] Qian, L. F., Batra, R. C., and Chen, L. M., "Static and Dynamic Deformations of Thick Functionally Graded Elastic Plates by Using Higher-Order Shear and Normal Deformable Plate Theory and Meshless Local Petrov-Galerkin Method," *Composites, Part B*,

Vol. 35, Nos. 6–8, Sept.–Dec. 2004, pp. 685–697.
doi:10.1016/j.compositesb.2004.02.004

[6] Mori, T., and Tanaka, K., "Average Stress in Matrix and Average Elastic Energy of Materials with Misfitting Inclusions," *Acta Metallurgica*, Vol. 21, No. 5, 1973, pp. 571–574.
doi:10.1016/0001-6160(73)90064-3

[7] Ramirez, F., Heyligher, P., and Pan, E., "Static Analysis of Functionally Graded Elastic Anisotropic Plates Using a Discrete Layer Approach," *Composites, Part B*, Vol. 37, No. 1, 2006, pp. 10–20.
doi:10.1016/j.compositesb.2005.05.009

[8] Pan, E., "Exact Solution for Functionally Graded Anisotropic Elastic Composite Laminates," *Journal of Composite Materials*, Vol. 37, No. 21, 2003, pp. 1903–1920.
doi:10.1177/0021998033035565

[9] Pagano, N. J., "Exact Solutions for Rectangular Bidirectional Composites and Sandwich Plates," *Journal of Composite Materials*, Vol. 4, No. 1, 1970, pp. 20–34.

[10] Pagano, N. J., "Exact Solutions for Composites Laminates in Cylindrical Bending," *Journal of Composite Materials*, Vol. 3, No. 3, 1969, pp. 398–411.
doi:10.1177/002199836900300304

[11] Vel, S. S., and Batra, R. C., "Three-Dimensional Exact Solution for the Vibration of Functionally Graded Rectangular Plates," *Journal of Sound and Vibration*, Vol. 272, Nos. 3–5, 2004, pp. 703–730.
doi:10.1016/S0022-460X(03)00412-7

[12] Vel, S. S., and Batra, R. C., "Three-Dimensional Analysis of Transient Thermal Stresses in Functionally Graded Plates," *International Journal of Solids and Structures*, Vol. 40, No. 25, 2003, pp. 7181–7196.
doi:10.1016/S0020-7683(03)00361-5

[13] Ferreira, A. J. M., Batra, R. C., Roque, C. M. C., Qian, L. F., and Martins, P. A. L. S., "Static Analysis of Functionally Graded Plates Using Third-Order Shear Deformation Theory and a Meshless Method," *Composite Structures*, Vol. 69, No. 4, 2005, pp. 449–457.
doi:10.1016/j.compstruct.2004.08.003

[14] Chi, S.-H., and Chung, Y.-L., "Mechanical Behavior of Functionally Graded Material Plates Under Transverse Load, Part 1: Analysis," *International Journal of Solids and Structures*, Vol. 43, No. 13, 2006, pp. 3657–3674.
doi:10.1016/j.ijsolstr.2005.04.011

[15] Chi, S.-H., and Chung, Y.-L., "Mechanical Behavior of Functionally Graded Material Plates Under Transverse Load, Part 2: Numerical Results," *International Journal of Solids and Structures*, Vol. 43, No. 13, 2006, pp. 3675–3691.
doi:10.1016/j.ijsolstr.2005.04.010

[16] Ramirez, F., Heyligher, P., and Pan, E., "Discrete Layer Solution to Free Vibrations of Functionally Graded Magneto-Electro-Elastic Plates," *Mechanics of Advanced Materials and Structures*, Vol. 13, No. 3, 2006, pp. 249–266.
doi:10.1080/15376490600582750

[17] Carrera, E., "A Class of Two Dimensional Theories for Multilayered Plates Analysis," *Atti Accademia delle Scienze di Torino, Memorie Scienze Fisiche*, Vols. 19–20, 1995, pp. 49–87.

[18] Carrera, E., "Theories and Finite Elements for Multilayered Anisotropic, Composite Plates and Shells," *Archives of Computational Methods in Engineering*, Vol. 9, No. 2, 2002, pp. 87–140.

[19] Carrera, E., and Demasi, L., "Multilayered Finite Plate Element Based on Reissner Mixed Variational Theorem, Part 1: Theory," *International Journal for Numerical Methods in Engineering*, Vol. 55, 2002, pp. 191–231.
doi:10.1002/nme.492

[20] Carrera, E., and Demasi, L., "Multilayered Finite Plate Element Based on Reissner Mixed Variational Theorem, Part 2: Numerical Analysis," *International Journal for Numerical Methods in Engineering*, Vol. 55, 2002, pp. 253–291.

[21] Carrera, E., "An Assessment of Mixed and Classical Theories for Thermal Stress Analysis of Orthotropic "Multilayered" Plates," *Journal of Thermal Stresses*, Vol. 23, No. 9, Dec. 2000, pp. 797–831.
doi:10.1080/014957300750040096

[22] Robaldo, A., and Carrera, E., "Mixed Finite Elements for Thermoelastic Analysis of Multilayered Anisotropic Plates," *Journal of Thermal Stresses*, Vol. 30, No. 2, Feb. 2007, pp. 165–194.
doi:10.1080/01495730600897385

[23] Robaldo, A., Carrera, E., and Benjeddou, A., "A Unified Formulation for Finite Element Analysis of Piezoelectric Adaptive Plates," *Computers and Structures*, Vol. 84, Nos. 22–23, Sept. 2006, pp. 1494–1505.
doi:10.1016/j.compstruc.2006.01.029

[24] Carrera, E., and Brischetto, S., "Reissner Mixed Theorem Applied to Bending Analysis of Piezoelectric Shells," *Journal of Intelligent Material Systems and Structures*, Vol. 18, Oct. 2007, pp. 1083–1107

[25] Carrera, E., and Brischetto, S., "Piezoelectric Shells Theories with a Priori Continuous Transverse Electromechanical Variables," *Journal of Mechanics of Materials and Structures*, Vol. 2, No. 2, Feb. 2007, pp. 377–399.

[26] Batra, R. C., and Aimmanee, S., "Missing Frequencies in Previous Exact Solutions of Free Vibrations of Simply Supported Rectangular Plates," *Journal of Sound and Vibration*, Vol. 265, No. 10, Aug. 2003, pp. 887–896.
doi:10.1016/S0022-460X(02)01568-7

[27] Aimmanee, S., and Batra, R. C., "Analytical Solution for Vibration of an Incompressible Isotropic Linear Elastic Rectangular Plate, and Frequencies Missed in Previous Solutions," *Journal of Sound and Vibration*, Vol. 302, No. 3, May 2007, pp. 613–620.
doi:10.1016/j.jsv.2006.11.029

[28] Reissner, E., "On a Certain Mixed Variational Theory and a Proposed Application," *International Journal for Numerical Methods in Engineering*, Vol. 20, No. 7, 1984, pp. 1366–1368.
doi:10.1002/nme.1620200714

A. Palazotto
Associate Editor